YIELD OF RANDOM ELASTOPLASTIC MATERIALS

Wei Li and Martin Ostoja-Starzewski

YIELD OF RANDOM ELASTOPLASTIC MATERIALS

Wei Li and Martin Ostoja-Starzewski

When separation of scales in random media does not hold, the representative volume element (RVE) of deterministic continuum mechanics does not exist in the conventional sense, and new concepts and approaches are needed. This subject is discussed here in the context of microstructures of two types – planar random chessboards, and planar random inclusion-matrix composites – with microscale behavior of the elastic-plastic-hardening (power-law) variety. The microstructures are assumed to be spatially homogeneous and ergodic. Principal issues under consideration are yield and incipient plastic flow of statistical volume elements (SVE) on mesoscales, and the scaling trend of SVE to the RVE response on the macroscale. Indeed, the SVE responses under uniform displacement (or traction) boundary conditions bound from above (or below, respectively) the RVE response. We show through extensive simulations of plane stress that the larger the mesoscale, the tighter are both bounds. However, mesoscale flows under both kinds of loading do not generally display normality. Also, within the limitations of currently available computational resources, we do not recover normality (or even a trend towards it) when studying the largest possible SVE domains.

1. Introduction

For over a century, plasticity of materials has principally been studied from a homogeneous continuum perspective, where the deterministic response of a Representative Volume Element (RVE) was assumed a priori. The past two decades have seen an increasing focus on determination of effective plastic response from micromechanical considerations, albeit without much consideration of the finite-size-scaling to the RVE, for example, [Castaneda and Suquet 1997]. However, if one considers such a scaling, one must look at one or both of the following: stochastic responses below the RVE level, and the solution of plasticity problems where the random field is of finite extent. In the first case, one has to work with a Statistical Volume Element (SVE) defined over an ensemble of specimens not large enough to be the RVE, while in the second case one has to revisit various boundary value problems of plasticity (such as a punch on a half-space) in a random field setting. The RVE is set up on a macroscale, while the SVE is set up on a mesoscale. Reviews of all these issues have recently been presented by [Ostoja-Starzewski 2005; 2006].

Note that most micromechanics studies aim at determining the effective constitutive properties at the RVE level without clearly specifying the RVE size. Many studies obviate the entire problem by simply postulating a fictitious periodic microstructure, and directly identifying the periodic cell as the RVE. To introduce scale effects, consider Figure 1, which shows two different types of model random media, both much smaller than the RVE. It is convenient here to use a dimensionless scale parameter $\delta (= L/d)$ to characterize the mesoscale. Here d is the heterogeneity size, that is, an inclusion's diameter, and L is the

Keywords: random media, scale effects, plasticity, RVE, homogenization.

mesoscale size. As we pass from the mesoscale (δ finite) to macroscale (δ infinite), the RVE is obtained, and the question is: at what δ does RVE apply? Clearly, $\delta = \infty$ is impractical, but perhaps a response close to RVE can be attained on a relatively small mesoscale.

In this study we focus on the passage from SVE to RVE. If that passage—effectively, a scale dependence of constitutive response—displays a clear trend in a specified sense, we say that the RVE can be approximated within a certain error on a specific length scale. Our approach follows the first study in [Jiang et al. 2001], and is a particular case of a general methodology to assess RVE size [Huet 1990; Sab 1992] in elasticity and inelasticity in the sense of [Hill 1963], and to set up micromechanically-based random fields of continuum properties [Ostoja-Starzewski and Wang 1989; Ostoja-Starzewski 1994]. This approach has primarily been used in linear elasticity [Hazanov and Huet 1994; Cluni and Gusella 2004; Kanit et al. 2003; Ostoja-Starzewski 1999; 2000], and in new inroads in viscoelasticity [Huet 1995; 1999], elastoplasticity [Jiang et al. 2001; Ostoja-Starzewski 2005], plasticity with damage [Clayton and McDowell 2004], thermomechanics with internal variables [Ostoja-Starzewski 2002], and finite (thermo)elasticity [Khisaeva and Ostoja-Starzewski 2006]. Related studies in linear thermoelasticity and Stokesian flow in porous media are currently underway [Du and Ostoja-Starzewski 2006a; 2006b]. For elastic-perfectly plastic materials, similar results have been obtained by [He 2001] using a mathematically more rigorous analysis involving gauge functions.

Using this approach, it has already been shown that the effective plastic response of a random material with a statistically homogeneous and ergodic microstructure can be bounded from above and below by responses obtained under uniform kinematic and traction boundary conditions, respectively, applied to finite size domains. This procedure leads to scale-dependent hierarchies of upper and lower bounds, which converge, as the scale tends to infinity, towards the RVE. In particular, we present a computational mechanics study of yield and incipient plastic flow of SVE, and the aforementioned trend to the RVE, for two kinds of model planar random materials in plane stress: a random two-phase chessboard (Figure 1 (a, b)), and a matrix-inclusion composite (Figure 1 (c, d)). We also examine scale dependence of the flow rule, to determine whether normality holds. We find that even though each phase alone possesses normality, the mesoscale flow rule, in general, does not.

2. Model Formulation

2.1. *Random material.* The formulation of deterministic continuum mechanics involves a tacit assumption—the so-called *separation of scales*:

$$d < L \ll L_{\text{macro}}, \tag{2-1}$$

where d is the microscale (e.g., typical grain size), L is the size of RVE, and L_{macro} is the macro size which usually is assumed to be much larger than the RVE. The size of RVE, L, relative to d is not known a priori. That is why, to be on the safe side, the left inequality in Equation (2–1) is often replaced with $\ll$. Thus, the establishment of L/d for which the RVE may actually be adopted with a certain accuracy (of, say, 10%), is of key interest. Consistent with the methodology of our previous studies, we use a dimensionless number

$$\delta = L/d \geq 1$$

to denote the mesoscale.

In two dimensions, we work with square-shaped mesoscale domains, with sides of length L, containing the microstructure of characteristic microscale d (inclusion diameter); see Figure 1. Following [Huet 1990], we sometimes call the mesoscale properties *apparent*, and reserve the term *effective* for the RVE level.

Specimens $B_\delta(\omega)$ are drawn from the ensemble $\mathbf{B} = \{B_\delta(\omega); \omega \in \Omega\}$, where Ω is a sample space. For any sample $B_\delta(\omega)$ of size δ taken from Ω, its properties are deterministic but different from each other due to the random nature of the medium. All samples $B_\delta(\omega)$ constitute the *ensemble* $\mathbf{B} = \{B_\delta(\omega); \omega \in \Omega\}$.

The ergodic property (or hypothesis) of the random field of a specific material property $\mathbf{F}$, such as the stiffness tensor $\mathbf{C}$, can be described as

$$\overline{\mathbf{F}(\omega)} \equiv \lim_{L \to \infty} \frac{1}{L} \int_0^L \mathbf{F}(\omega, x) dx = \int_\Omega \mathbf{F}(\omega, x) dP(\omega) \equiv \langle \mathbf{F}(x) \rangle.$$

Here the overbar indicates the volume average, while $\langle\ \rangle$ stands for the ensemble average, whereby $P(\omega)$ is the probability measure assigned to the ensemble $\{\mathbf{F}(\omega, x); \omega \in \Omega, x \in X\}$. In practice, we use

$$\overline{\mathbf{F}(\omega)} \equiv \frac{1}{M} \sum_{m=1}^M \mathbf{F}(\omega, x_m) = \frac{1}{N} \sum_{n=1}^N \mathbf{F}(\omega_n, x) \equiv \langle \mathbf{F}(x) \rangle,$$

where M denotes the finite number of sampling points over one realization ω, and N denotes the finite number of realizations ω_n at one sampling point.

For materials with statistically homogeneous and ergodic properties, the mesoscale properties should be obtained by taking the ensemble average over $\mathbf{B}$. Usually, the smaller the sample size δ, the larger the number of samples which should be taken. When the window size δ approaches ∞, the mesoscale properties of any specimen $B_\delta(\omega)$ in $\mathbf{B}$ should be identical and same as effective properties.
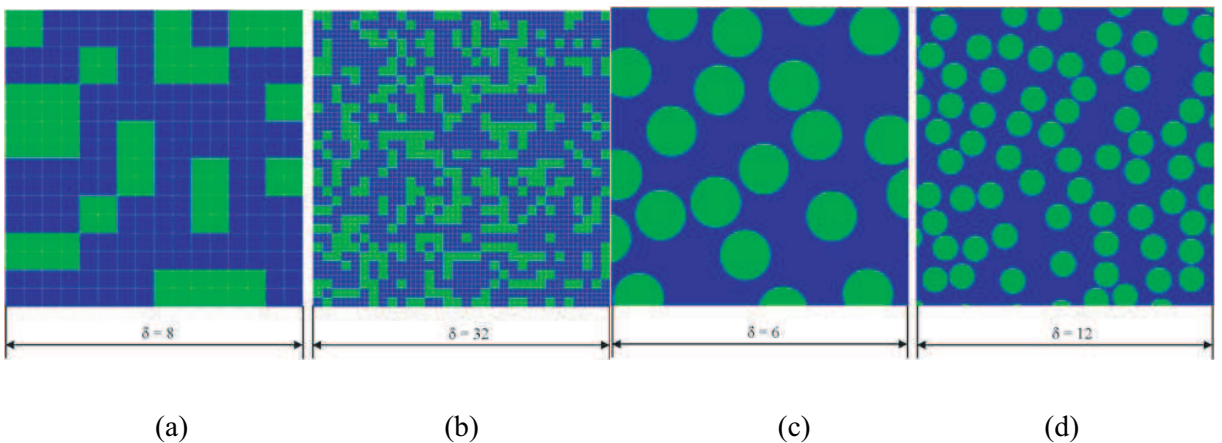

(a) (b) (c) (d)

Figure 1. Realizations of random chessboard and matrix-inclusion materials on two mesoscales at a nominal volume fraction 35%. Blue pertains to a hard phase, and green to a soft one. (a) $\delta = 8$, chessboard; (b) $\delta = 32$, chessboard; (c) $\delta = 6$, matrix-inclusion; (d) $\delta = 12$, matrix-inclusion.

2.2. *Boundary conditions.* For linear elastic heterogeneous materials, the necessary and sufficient condition of the equivalence between energetically and mechanically defined effective properties is contained in the well-known Hill condition [Hill 1963]

$$\overline{\boldsymbol{\sigma} : \boldsymbol{\varepsilon}} = \bar{\boldsymbol{\sigma}} : \bar{\boldsymbol{\varepsilon}} \ . \tag{2-2}$$

[Hazanov 1998] generalized Equation (2–2) to nonlinear heterogeneous materials as

$$\overline{\int \boldsymbol{\sigma} : d\boldsymbol{\varepsilon}} = \int \bar{\boldsymbol{\sigma}} : d\bar{\boldsymbol{\varepsilon}}.$$

For materials with perfect interfaces and no body forces, Equation (2–2) becomes

$$\int_{\partial B_\delta} (\boldsymbol{t} - \bar{\boldsymbol{\sigma}} \cdot \boldsymbol{n}) \cdot (\boldsymbol{u} - \bar{\boldsymbol{\varepsilon}} \cdot \boldsymbol{x}) dS = 0.$$

where $\boldsymbol{t}$ is the traction vector, $\boldsymbol{u}$ is the displacement vector on the specimen boundary ∂B_δ, $\boldsymbol{n}$ is the exterior unit normal vector, and $\boldsymbol{x}$ is the coordinate vector. The above equation clearly shows that among the solutions of the Hill condition one can identify three important types of boundary conditions:

(1) *uniform kinematic* boundary condition (UKBC, also known as *displacement*, *essential* or *Dirichlet*)

$$\boldsymbol{u}(\boldsymbol{x}) = \boldsymbol{\varepsilon}^0 \cdot \boldsymbol{x}, \quad \text{for all } \boldsymbol{x} \in \partial B_\delta, \tag{2-3}$$

(2) *uniform static* boundary condition (USBC, also known as *traction*, *natural* or *Neumann*)

$$\boldsymbol{t}(\boldsymbol{x}) = \boldsymbol{\sigma}^0 \cdot \boldsymbol{n}, \quad \text{for all } \boldsymbol{x} \in \partial B_\delta, \tag{2-4}$$

(3) *uniform mixed-orthogonal* boundary condition (UMBC)

$$(\boldsymbol{t}(\boldsymbol{x}) - \boldsymbol{\sigma}^0 \cdot \boldsymbol{n}) \cdot (\boldsymbol{u}(\boldsymbol{x}) - \boldsymbol{\varepsilon}^0 \cdot \boldsymbol{x}) = 0, \quad \text{for all } \boldsymbol{x} \in \partial B_\delta. \tag{2-5}$$

In studies of scale effects thus far, most research has been done in terms of the first two cases since these provide, respectively, upper bounds and lower bounds for the effective properties. In common engineering practice, however, the UKBC and USBC loadings can be very difficult to realize. Interestingly, most laboratory and industrial testing is done under loadings closer to the mixed-orthogonal boundary condition in Equation (2–5).

2.3. *Constitutive laws for elastic-plastic-hardening materials.* For elastic-plastic-hardening materials, the constitutive responses of both phases $p(= 1, 2)$ are taken in the form [Hill 1950]

$$\begin{aligned}
d\varepsilon'_{ij} &= \frac{d\sigma'_{ij}}{2G_p} + h \cdot df_p \cdot \frac{\partial f_p}{\partial \sigma_{ij}} \quad \text{when } f_p = c_p \text{ and } df_p \geq 0, \\
d\varepsilon'_{ij} &= d\sigma'_{ij}/2G_p \quad \text{when } f_p < c_p, \\
d\varepsilon &= d\sigma \cdot \frac{(1 - 2v_p)}{2G_p(1 + v_p)} \quad \text{where } \left(d\varepsilon = \frac{d\varepsilon_{ii}}{3}, d\sigma = \frac{d\sigma_{ii}}{3} \right),
\end{aligned} \tag{2-6}$$

where primes indicate deviatoric tensor components. In Equation (2–6) G_p is a shear modulus, v_p is a Poisson's ratio, f_p is a yield function, and c_p is a material constant. For von Mises–Huber materials

with associated flow rule and isotropic hardening, the yield surface is defined as

$$f_p = \sqrt{\frac{3}{2}\sigma'_{ij}\sigma'_{ij}} = c_p.$$

As is well known, the von Mises–Huber yield surface in the π-plane is that of a circle, and in the $\sigma_1\sigma_2$-plane, is an ellipse. The flow rule (that is, the plastic strain direction) is described as

$$d\varepsilon^p_{ij} = d\lambda \cdot C \cdot \frac{\partial f}{\partial \sigma_{ij}} = d\lambda \cdot \frac{3}{2} \frac{\sigma'_{ij}}{\sqrt{\frac{3}{2}\sigma'_{kl}\sigma'_{kl}}}. \tag{2–7}$$

Since $f(\sigma_{ij}) = $ constant on the yield surface, $\frac{\partial f}{\partial \sigma_{ij}}$ must be normal to that surface; therefore, the plastic strain vector is normal to the yield locus.

2.4. *Hierarchy of mesoscale bounds of stress/strain response for elastoplastic random materials.* Under monotonically increasing loading, the elastoplastic hardening composites can be treated as physically nonlinear elastic materials. Using the variational principles, one can obtain

$$\langle w(\varepsilon^0, \infty) \rangle \leq \langle w(\varepsilon^0, \delta) \rangle \leq \langle w(\varepsilon^0, \delta') \rangle \leq \langle w(\varepsilon^0, 1) \rangle \equiv w^V, \ 1 < \delta' < \delta < \infty$$

$$\langle w^*(\sigma^0, \infty) \rangle \leq \langle w^*(\sigma^0, \delta) \rangle \leq \langle w^*(\sigma^0, \delta') \rangle \leq \langle w^*(\sigma^0, 1) \rangle \equiv w^{*R}, \ 1 < \delta' < \delta < \infty$$

here $w(\varepsilon^0, \delta)$ and $w^*(\sigma^0, \delta)$ — obtained by Equations (2–3) and (2–4), respectively — represent the volume average strain energy and complementary energy densities of an arbitrary window of size δ that may be placed anywhere in the material domain of any random sample. w^V and w^{*R} are the Voigt and Reuss bounds respectively.

Since the stiffness and compliance tensors are no longer constant any more, we now consider the tangent stiffness and compliance moduli (C^{Td}_δ or S^{Tt}_δ), which are defined as

$$\overline{d\boldsymbol{\sigma}} = \boldsymbol{C}^{Td}_\delta : \overline{d\boldsymbol{\varepsilon}} = \boldsymbol{C}^{Td}_\delta : d\boldsymbol{\varepsilon}^0; \quad \overline{d\boldsymbol{\varepsilon}} = \boldsymbol{S}^{Tt}_\delta : \overline{d\boldsymbol{\sigma}} = \boldsymbol{S}^{Tt}_\delta : d\boldsymbol{\sigma}^0,$$

where superscript d (or t) indicates that the response is obtained under the displacement (or traction) boundary condition. Finally, there is a hierarchy of bounds on the effective tangent modulus for a linear comparison solid: [Jiang et al. 2001; Ostoja-Starzewski 2005]

$$\langle \boldsymbol{S}^{TS}_1 \rangle^{-1} \equiv \langle \boldsymbol{S}^{Tt}_1 \rangle^{-1} \leq \cdots \leq \langle \boldsymbol{S}^{Tt}_{\delta'} \rangle^{-1} \leq \langle \boldsymbol{S}^{Tt}_\delta \rangle^{-1} \leq \cdots \leq \left(\boldsymbol{S}^T_\infty \right)^{-1}$$

$$\equiv \boldsymbol{C}^T_\infty \leq \cdots \leq \langle \boldsymbol{C}^{Td}_\delta \rangle \leq \langle \boldsymbol{C}^{Td}_{\delta'} \rangle \leq \cdots \leq \langle \boldsymbol{C}^{Td}_1 \rangle \tag{2–8}$$

$$\equiv \langle \boldsymbol{C}^{TT}_1 \rangle, \quad \text{for all } \delta' < \delta \leq \infty,$$

where $\langle \boldsymbol{s}^{TS}_1 \rangle^{-1}$ and $\langle \boldsymbol{c}^{TT}_1 \rangle$ are the Sachs and Taylor bounds, respectively.

2.5. *Hierarchy of mesoscale yield surface bounds for elastoplastic random materials.* To study the mesoscale yield surface, one must first define the mesoscale yield condition for a specimen. Due to the heterogeneity of the material, stress distribution is nonuniform under uniform loading, which leads the local stress to reach the yield stress level somewhere in the material domain, even though the volume average stress is far lower than the yield stress of the material. Obviously, it would not be reasonable

Material parameters	ε_0	σ_0 (MPa)	N	E (GPa)	υ
Soft phase	1.036e-3	75	0.25	72.4	0.33
Hard phase	1.425e-3	295	0.15	207	0.32

Table 1. Material parameters.

to define the yield condition of a sample as the stress level when the first yield occurs in the specimen. [Dvorak and Bahei-El-Din 1987] proposed a bimodal plasticity theory for heterogeneous composites where both the fiber and the matrix participate in carrying the applied load. According to this theory, the overall yield of a sample indicates magnitudes of the overall stress which causes local volume average stress to satisfy the yield condition in any phase.

For von Mises–Huber materials, the mesoscale yield condition of the composite in the overall stress space Σ is defined as

$$F_\delta(\Sigma) = \inf \left\{ \Sigma \in R^{3\times3} \mid \exists \sigma(x) \text{ with } \bar{\sigma} = \Sigma, f_p(K_p \Sigma) = c_p, \quad \text{for all } x \in B_\delta, p = 1, 2 \right\}, \quad (2\text{–}9)$$

where K_p is the mechanical stress concentration factor, with (6×6) matrices, and Σ is treated as a (6×1) vector.

For a rigid-perfectly-plastic material, the hierarchy of inclusions for mesoscale yield surfaces is given in [Ostoja-Starzewski 2005] as

$$D_1^d \supseteq \cdots \supseteq D_{\delta'}^d \supseteq D_\delta^d \supseteq \cdots \supseteq D_\infty^d \equiv D_\infty^t \supseteq \cdots \supseteq D_\delta^t \supseteq D_{\delta'}^t \supseteq \cdots \supseteq D_1^t, \quad \text{for all } \delta' = \delta/2, \quad (2\text{–}10)$$

where D_δ denotes a domain in stress space bounded by an ensemble average yield surface $\langle F_\delta \rangle$. Without proof, we now conjecture that in an elastoplastic problem, the same type of hierarchy holds based on the definition (2–9). We confirm this conjecture through computations in Section 3.5.

2.6. *The flow rule for elastoplastic random materials.* The flow rule in Equation (2–7) pertains to homogeneous materials. However for heterogeneous materials, it is not at all clear that the normality rule (that is, the associated flow rule) still holds on mesoscales. In fact, it is still an open issue whether the normality rule is recovered computationally at the RVE level, that is, whether

$$d\varepsilon_{ij}^p = d\lambda \cdot C \cdot \frac{\partial f}{\partial \sigma_{ij}} \qquad \text{or} \qquad d\varepsilon_{ij}^p \neq d\lambda \cdot C \cdot \frac{\partial f}{\partial \sigma_{ij}}. \qquad (2\text{–}11)$$

3. Computational mechanics of two random materials

3.1. *Models of two random materials.* We investigated two model two-phase composite materials. The first is a planar random chessboard, Figure 1 (a-b); the second one is a porous medium generated by placing circular disks whose centers come from a planar hard-core Poisson point field, Figure 1 (c-d). In both cases, the volume fraction of hard phases is 0.35. The *hard core* condition means that no two disks may touch. In fact, in order to avoid narrow-neck effects in the fluid field, the minimum distance between disk centers is set at 1.1 times the diameter of the disk.
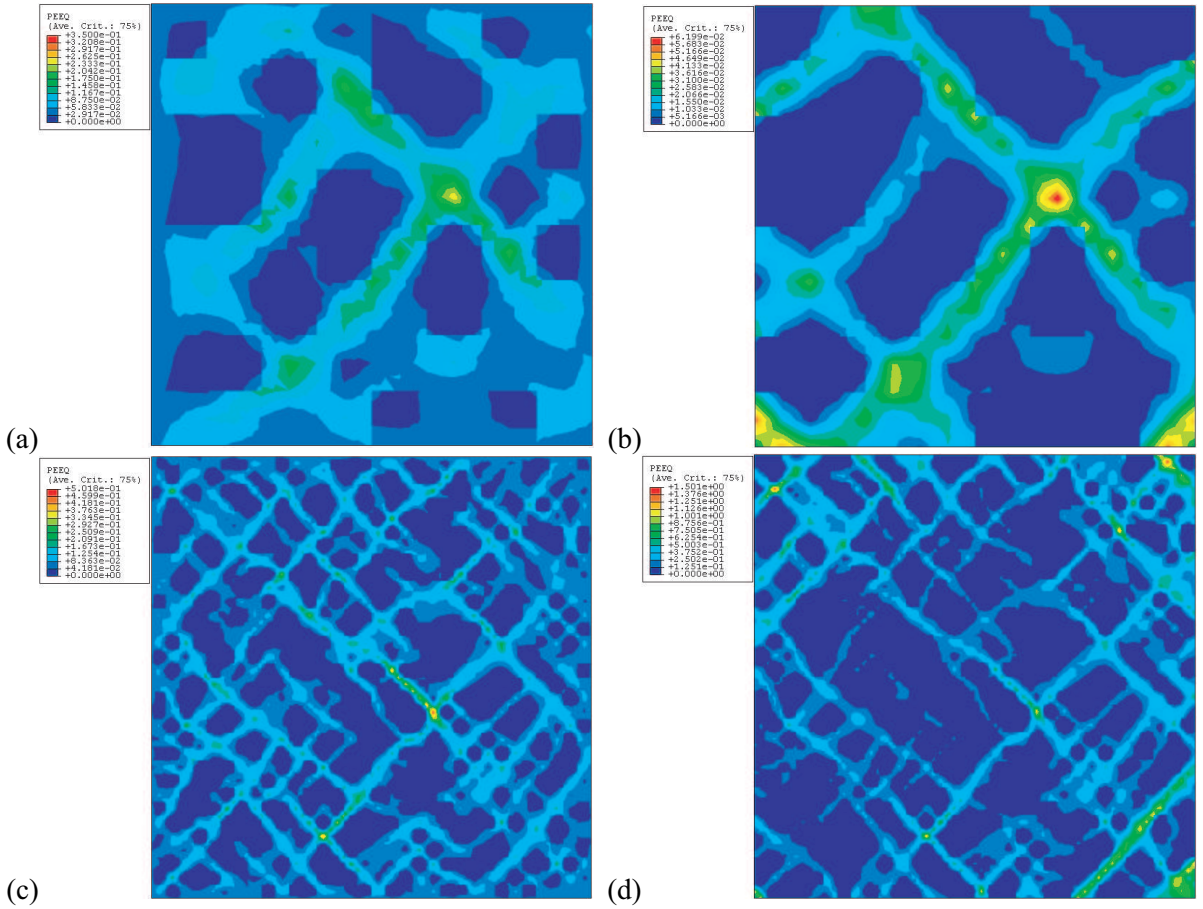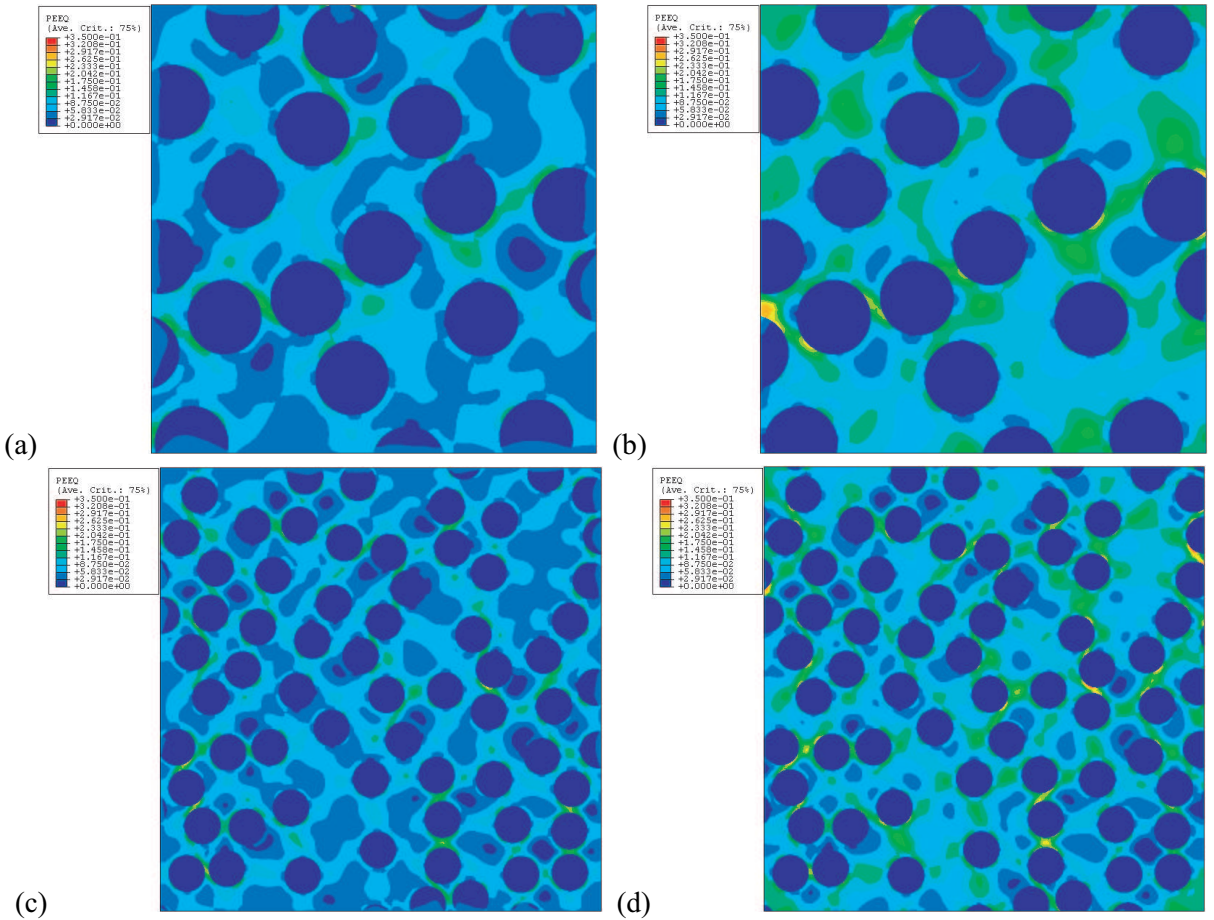
Figure 2. Contour plots of equivalent plastic strain for windows shown in Figure 1 (a, b) under different boundary conditions: (a, c) displacement; (b, d) traction.

A numerical analysis of composite materials shown in Figure 1, in plane stress, is carried out using ABAQUS. The interface between two phases is assumed to be perfect bonding, i.e. there is no phase-separation and no slip at interphase boundary. The stress-strain response is characterized by a piece-wise power law [Dowling 1993]

$$i\sigma/\sigma_0 = \begin{cases} \varepsilon/\varepsilon_0, & \text{if } \varepsilon \leq \varepsilon_0, \\ (\varepsilon/\varepsilon_0)^N, & \text{else.} \end{cases}$$

The material parameters are given in Table 1. The von Mises–Huber yield criterion, with associated flow rule, is assumed for each phase. Shear loading is applied through one of two types of uniform boundary conditions:

$$\text{UKBC: } \varepsilon_{11}^0 = -\varepsilon_{22}^0 = \varepsilon, \varepsilon_{12}^0 = 0 \quad \text{or} \quad \text{USBC: } \sigma_{11}^0 = -\sigma_{22}^0 = \sigma, \sigma_{12}^0 = 0. \tag{3-1}$$

Here the prescribed stress and strain are ~ 0.04 and $\sim 1.75e8$ Pa, respectively. The UMBC is not being used.

Figure 3. Contour plots of equivalent plastic strain for window shown in Figure 1 (c, d)
under different boundary conditions: (a, c) displacement; (b, d) traction.

The mesoscale yield detection condition follows Equation (2–9) and involves an equality between the
average stress of the soft phase and the yield stress of that phase within a 3.5% error.

3.2. *Patterns of shear bands.* The equivalent plastic strain (PEEQ) contours for differing window sizes
of δ under differing boundary conditions are shown in Figure 2 for chessboard material, and in Figure 3
for the matrix-inclusion composite. Although the shear bands differ somewhat for the two types of
material, clearly, we can see the following common characteristics:

- The shear bands are irregular, but conform to the actual spatial distribution of the material mi-
  crostructure.

- The shear bands are roughly 45° from the principal axes of tensile loading.

- For a small window size of, say, $\delta = 8$, some shear bands can cross the entire window, but for a
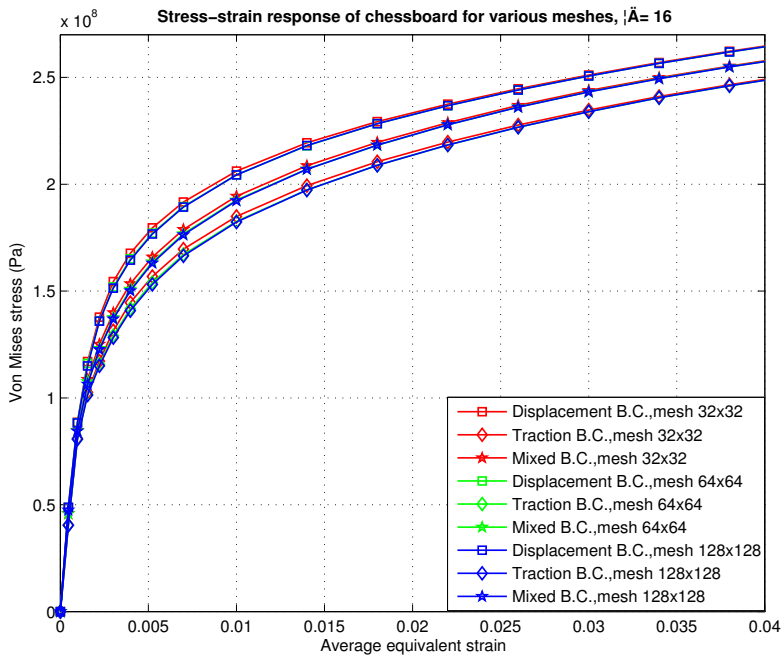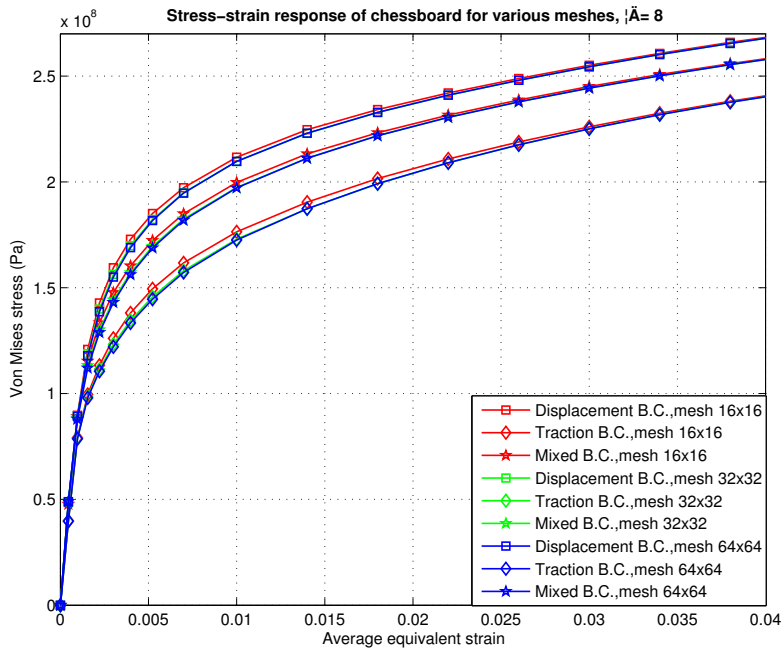 large window size, $\delta = 32$, almost no shear band can do so.

Figure 4. Comparison of ensemble average stress-strain responses of chessboard composites for various meshes: (a) $\delta = 8$; (b) $\delta = 16$.
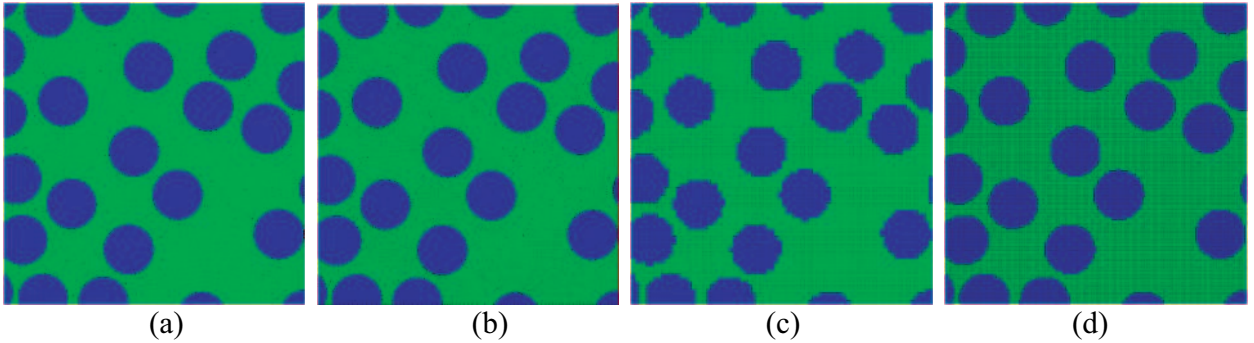
Figure 5. Comparison of different meshes for matrix-inclusion composites at $\delta = 6$: (a) coarse mesh, global mesh size $= 1.0$; (b) fine mesh, global mesh size$= 0.5$; (c) uniform grid, mesh 80×80; (d) uniform grid, mesh 160×160.

- The shear band patterns are different under different boundary conditions, and seem to rank in the following order for stress concentration factors: displacement and traction.

3.3. *Effects of mesh refinement.*

3.3.1. *Chessboard model.* Figure 4 shows that all the stress-strain curves shift down with the increasing refinement of mesh, because introducing more finite elements furnishes more degrees of freedom. In particular, we notice that the shift when the mesh changes from 4×4 to 8×8 for each inclusion is much smaller than when the mesh changes from 2×2 to 4×4, which means that the effect of mesh refinement tends to vanish at 8×8.

3.3.2. *Matrix-inclusion model.* There are two types of mesh in the FE method: uniform and nonuniform. For uniform mesh, to approximate the complex geometry, a very large number of elements is needed, which requires more computational resources. Figure 5 (c) and (d) demonstrates grid refinements leading to improvement in the accuracy of a numerical simulation. The disadvantage of using uniform meshes is that the number of elements may become so large that, beyond a given window size δ, the computation becomes impractical.

The advantage of nonuniform mesh is that the mesh density can be adjusted according to a change of geometry, so it can greatly reduce the number of nodes while maintaining the same solution accuracy. Comparing the case of 6,400 (80×80) elements with that of 25,600 (160×160) elements in the uniform mesh—as shown in Figure 5 (c) and (d)—there are only 3,291 elements of the coarse mesh and 8,564 elements of the fine mesh, (see Figure 5 (a) and (b)). In addition, the nonuniform mesh geometry is more accurate than the uniform one.

Unlike to the chessboard composites, all the curves shift up with the increased mesh, but the shift is small and the curves almost overlap; see Figure 6. Since the area of the polygon inscribed into the circle is always smaller than that of the circle, the volume fraction of inclusions is always a little smaller than the real one, and this leads to very minor underestimates of material stiffness.

3.4. *Ensemble average stress-strain responses.* Figures 7 and 8 clearly show that with the increase in the mesoscale δ, the elastoplastic bounds obtained under kinematic and static boundary conditions
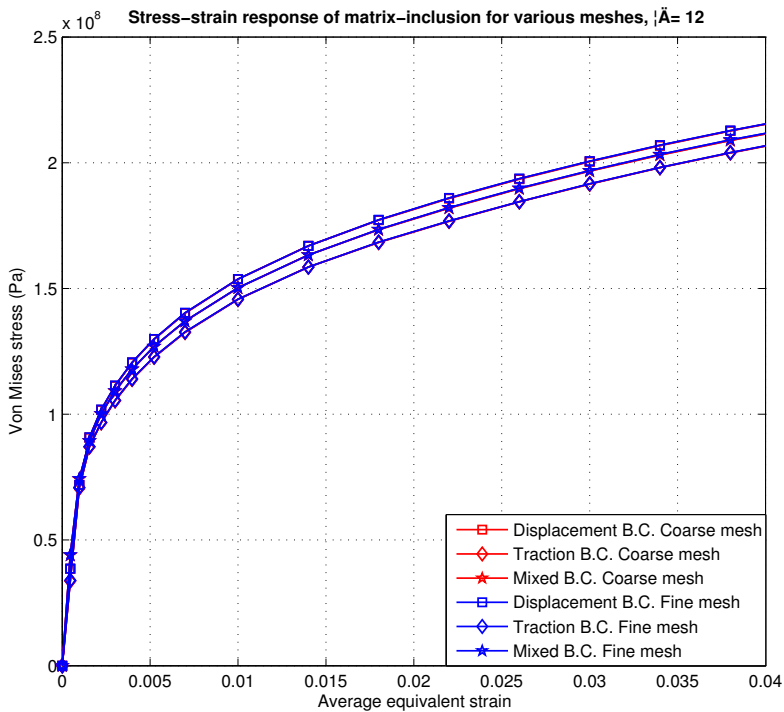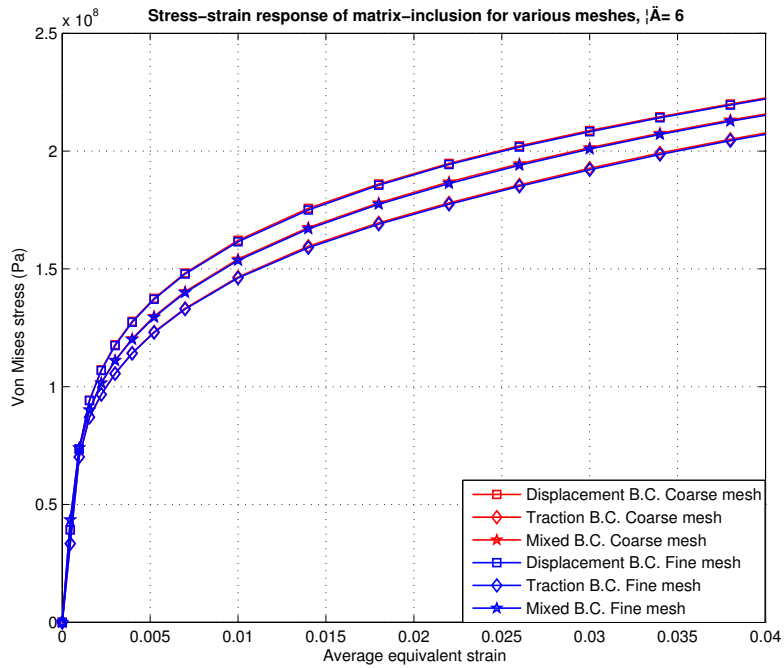
Figure 6. Comparison of ensemble average stress-strain responses of matrix-inclusion composites for differing meshes: (a) $\delta = 6$; (b) $\delta = 12$.
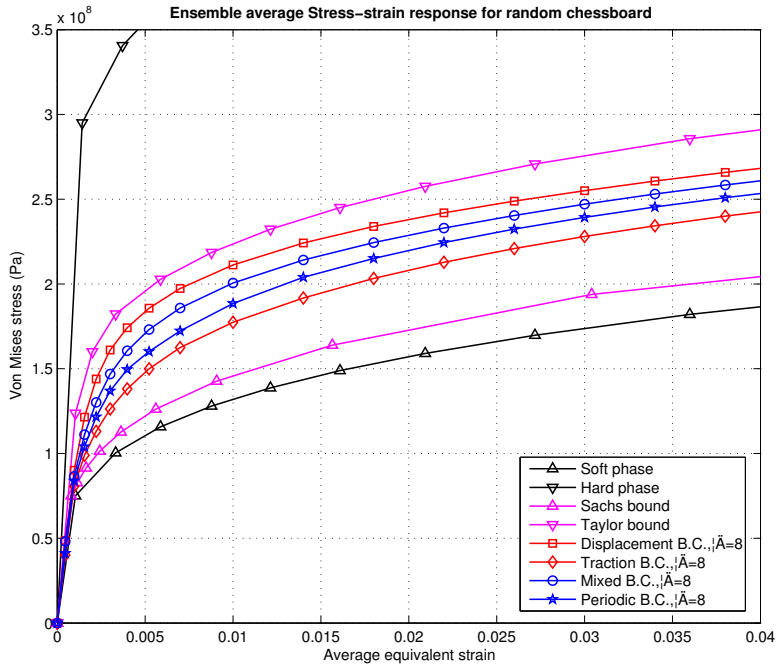
Figure 7. Ensemble average stress-strain responses for different mesoscales δ under various boundary conditions for the random chessboard. Responses of both constituent phases and the Sachs and Taylor bounds are also shown.

become tighter, while the slopes of curves, that is, the tangent moduli satisfy the relation described in Equation (2–8). For matrix-inclusion composites, one phenomenon we must consider is that the stress-strain curve can fall outside the Sachs bound, which is impossible for purely elastic materials. We can explain this by observing that, for the elastoplastic material, the stress concentration causes some local area or spot to yield which, in turn, softens the material. This is the result of the definition of yield (Equation (2–9)) employed here.

3.5. *Yield surfaces and flow rules.* To study the yield surface and the flow rule on mesoscales, we first introduce two different loading programs: displacement increment control and traction increment control. For the traction increment control

$$\Delta T = \Delta \Sigma \cdot n,$$

where ΔT is the increment of traction, and $\Delta \Sigma$ is the increment of volume average stress.

For the displacement increment control

$$\Delta U = \Delta E \cdot X,$$

where ΔU is the increment of displacement, ΔE is the increment of volume average strain.

For a specific load

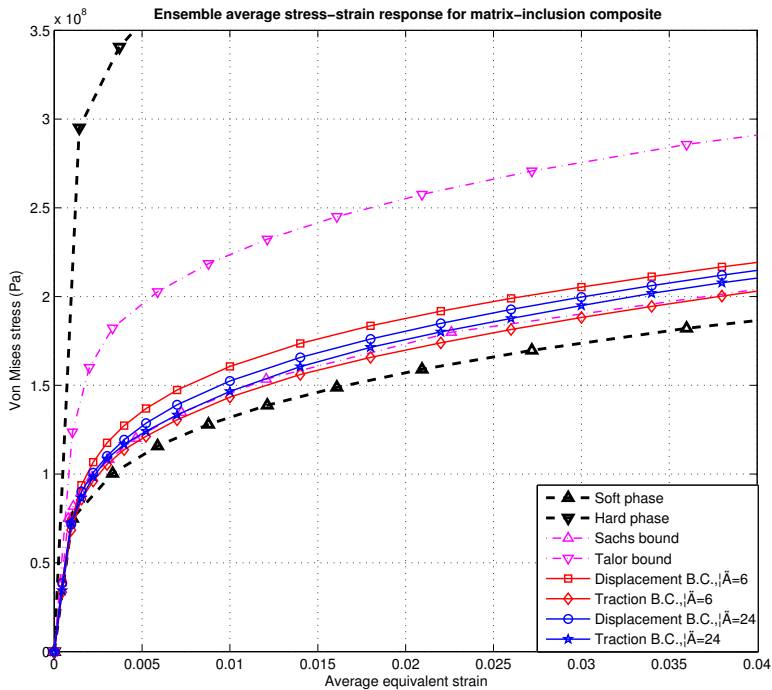$$E_1/E_2 = \text{const} \quad \text{or} \quad \Sigma_1/\Sigma_2 = \text{const}.$$

Figure 8. Ensemble average stress-strain responses for different mesoscales δ under various boundary conditions for the random matrix-inclusion composite. Also shown are the responses of both constituent phases as well as the Sachs and Taylor bounds.

In both loading programs, we fix the ratio of increment ($\Delta E_1 / \Delta E_2 = $ const or $\Delta \Sigma_1 / \Delta \Sigma_2 = $ const) and continue to increase it until the volume average stress Σ satisfies Equation (2–9). We then get one specific yield point.

The loading paths are shown in Figure 9. For each sample we applied 17 different loading paths corresponding to 17 different ratios of loading to obtain 17 yield points whose ratios (Σ_1 / Σ_2) vary from -1 to 1 (but only approximately so for displacement control). These 17 points cover quite densely one quarter of the yield surface, which, by symmetry arguments, is representative of the entire stress plane.

The loading paths are always linear for the traction increment control. However, for the displacement increment control, the loading paths are not linear since there are some areas or spots within the specimen yield due to local stress concentrations, even when the volume average stress is still lower than the yield stress; see Figure 9. For the chessboard composite, this phenomenon is even stronger than for the matrix-inclusion composite. Also, we can clearly see that the plastic strain rate is not always normal to the yield surface and the shape of yield surface is not perfectly elliptical.

Figure 10 depicts the scatter of yield locus of chessboard and matrix-inclusion composite materials for different window sizes of δ under traction and displacement boundary conditions. Obviously, the
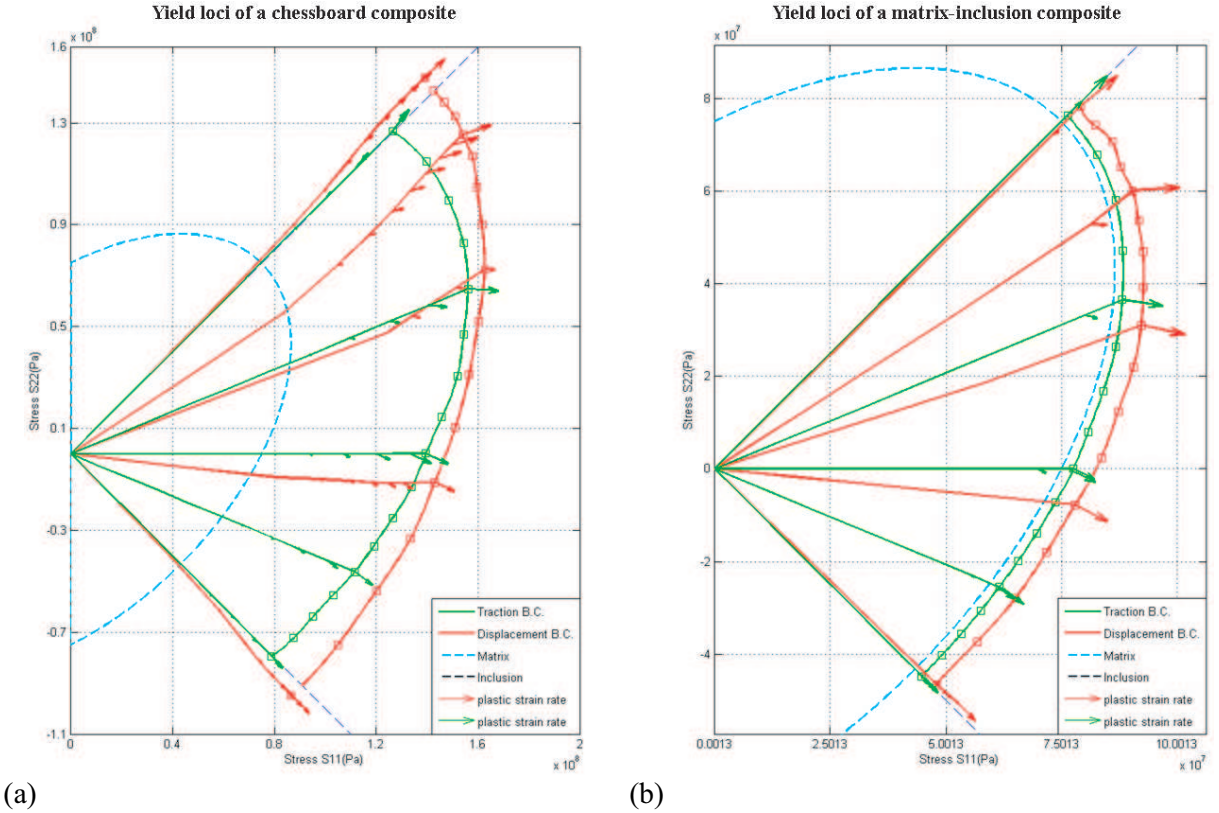
Figure 9. Yield surfaces and loading paths for one sample of (a) chessboard composite, $\delta = 8$, and (b) matrix-inclusion composite, $\delta = 6$.

smaller the window size, the higher the scatter; also the shape of the yield locus is more similar to an ellipse as the window size of δ increases.

Figure 11 shows the ensemble average yield surface on different mesoscales under two different loading controls. It shows that the mesoscale yield surfaces satisfy the hierarchy of inclusions conjectured in (2–10). Also with the increasing mesoscale δ, the yield surface bounds become tighter under displacement and traction boundary conditions.

Figure 12 shows the departure from normality of the plastic flow rate vector at mesoscale yield surfaces. We can infer that about 60% of yield surface is characterized by normality of plastic flow. Departure from normality occurs when the stress ratio Σ_{22}/Σ_{11} is around $0.3 \sim 0.9$, and is greater for the chessboard than for the matrix-inclusion composite.

3.6. *Why the loss of normality?* We base our understanding of normality in plasticity on the thermomechanics argument of Ziegler [1983], who points out the much more fundamental role played by the thermodynamic orthogonality in the space of velocities (that is, plastic strain rates). Only when the dissipation function Φ depends on velocities alone in its arguments will normality carry over to the space of dissipative stresses. When Φ depends also on other quantities, such as stresses or internal variables, normality is violated. For a disordered heterogeneous material, Φ is also a function of the
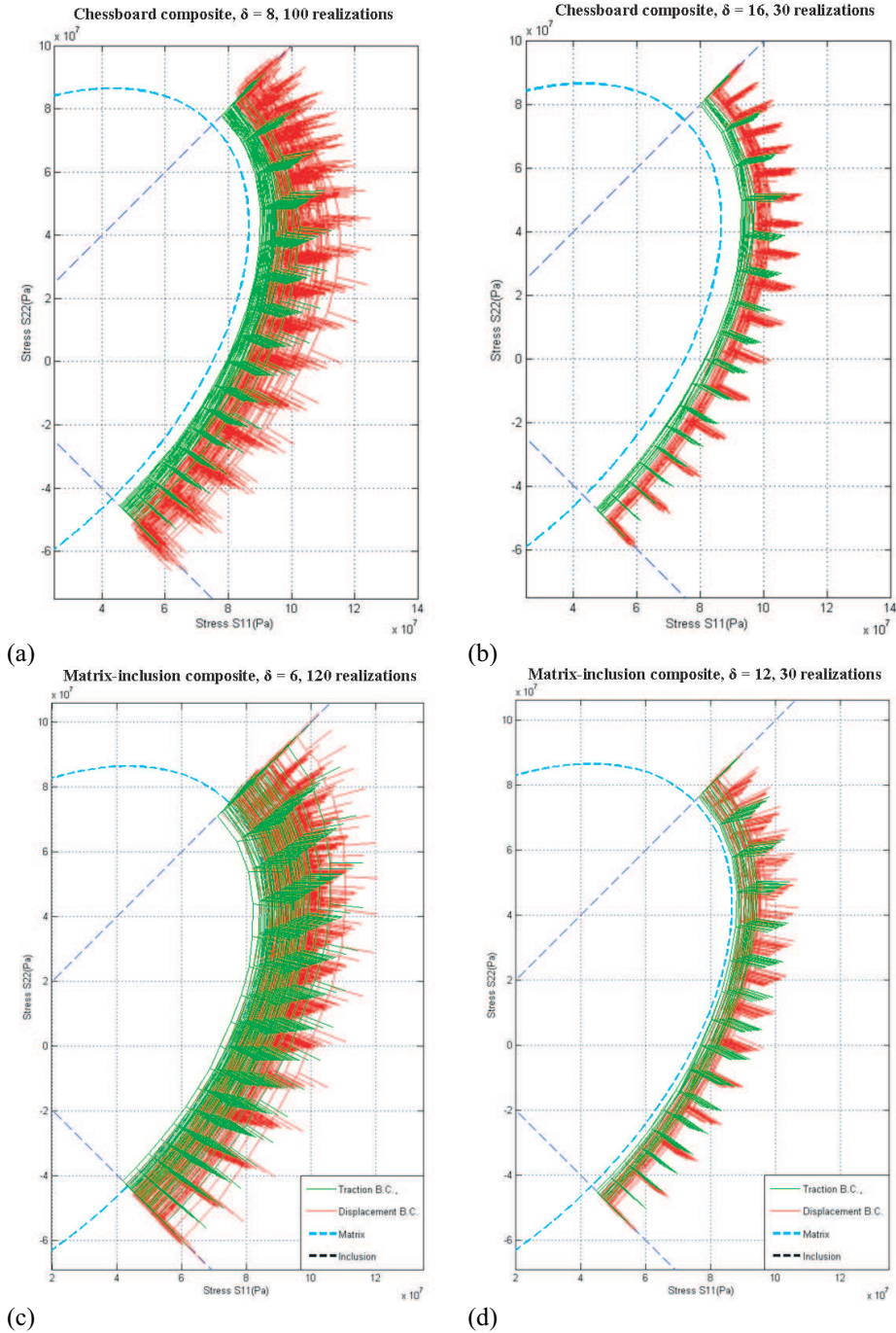
(a)

(b)

(c)

(d)

Figure 10. Scatter of yield locus under different boundary conditions for random materials: (a) chessboard composite at $\delta = 8$, 100 samples; (b) chessboard composite at $\delta = 16$, 30 samples; (c) matrix-inclusion composite at $\delta = 6$, 120 samples; (d) matrix-inclusion composite at $\delta = 12$, 30 samples.
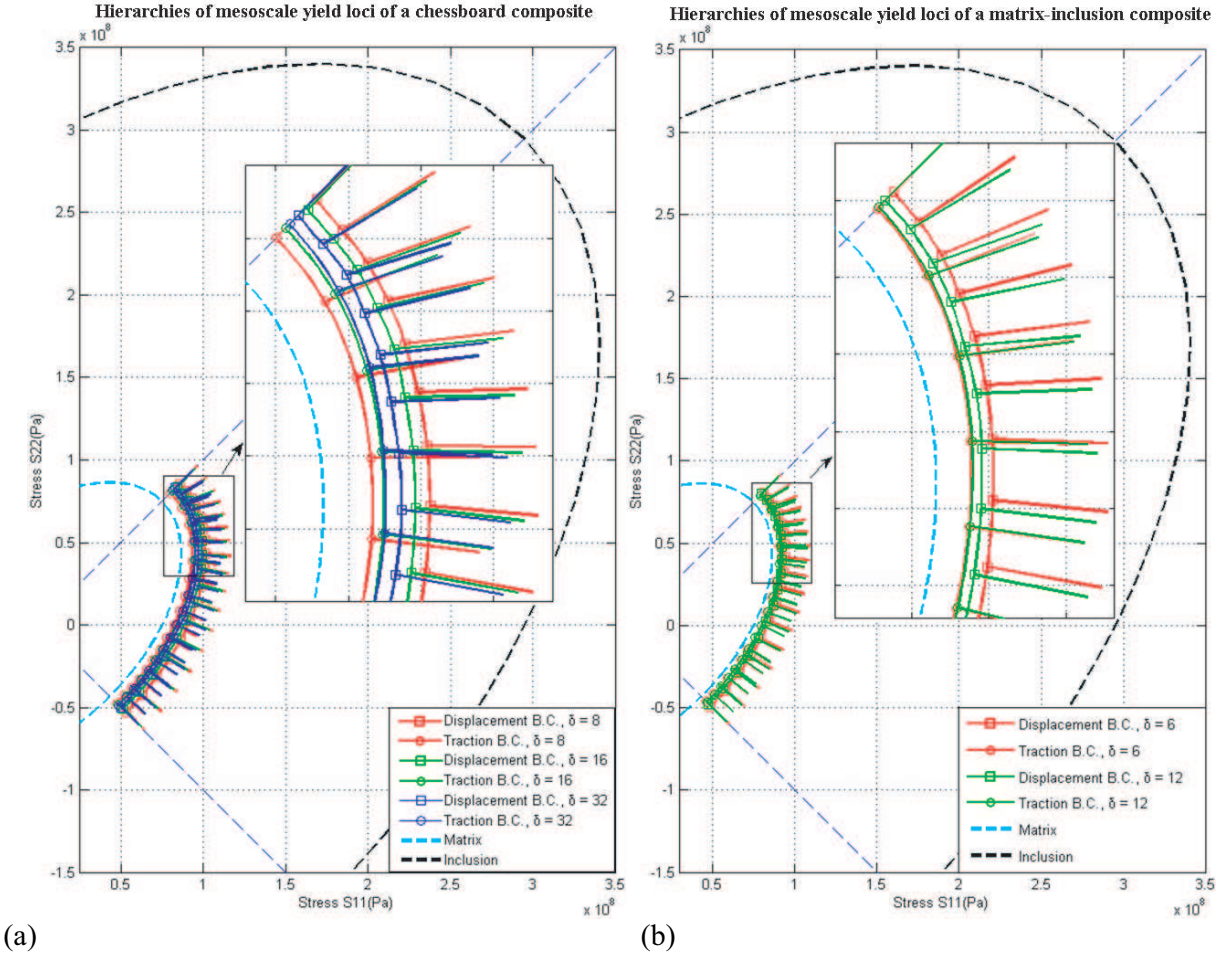
Figure 11. Hierarchy of (ensemble averaged) mesoscale bounds on RVE yield locus for (a) chessboard composite, and (b) matrix-inclusion composite.

specific microstructure, which may be represented by an internal variable α. This α must be chosen so that, for homogeneous material, it becomes null and the dependence of Φ on α vanishes. Thus, the simplest candidate for α may be the ratio of yield limits σ_0 of both phases. Other candidates are possible [Maugin 1998].

Another viewpoint refers to the classical result of nonlinear homogenization where the existence of a plasticity potential at the microlevel implies the existence of a macro-potential from which the effective constitutive equations are derived. The macro-potential is the mean value of the local potentials [Suquet 1997], so that the normality is preserved by a scale transition. In our study, according to Equation (2–9), macroyielding takes place as soon as local plastic flow begins for the first time at some point in the heterogeneous material. Such a macroyield criterion is not very useful in practical applications, but even for a more realistic (tolerant) yield criterion, the loss of normality would also persist under scale transition.
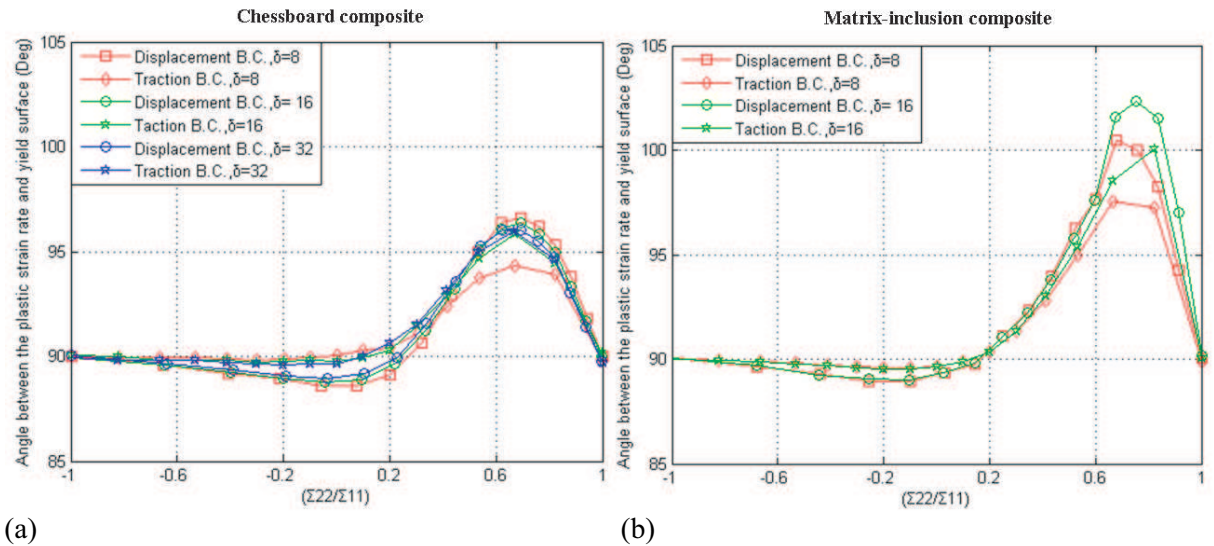
Figure 12. Departure from normality in mesoscale plastic flow under various boundary conditions on SVE for (a) chessboard composite and (b) matrix-inclusion composite.

4. Conclusions

We summarize the results of this study as follows:

1) We compute and verify the hierarchy of mesoscale stress-strain responses and the hierarchy of mesoscale yield surfaces for two models of elastoplastic-hardening random materials. The yield is studied employing the definition of yield point of [Dvorak and Bahei-El-Din 1987]. With this definition, mesoscale stress-strain responses under uniform traction boundary conditions may fall below the Sachs bound, although this occurs over a very small range of loading.

2) We find that mesoscale flow rule departs from normality under both uniform kinematic and traction boundary conditions. That departure is strongest when the ratio of two in-plane ensemble averaged principal stresses ranges from 0.3 to 0.9. Given the limitations of available computers, we cannot establish the expected trend to recover normality as the mesoscale domain (that is, SVE) grows and tends to the macroscale (RVE).

3) While we focus here on plane stress, very similar results have been found in plane strain.

Although our model materials have distinct and isotropic phases, our approach is also suited to analyze materials with piecewise-constant domains of anisotropic phases (polycrystals), and smoothly inhomogeneous media where no specific phase(s) can be distinguished. Fiber-structured paper is one example in the latter category [Ostoja-Starzewski and Castro 2003]. An extension to 3D problems is a matter of a far more extensive computational work.

Acknowledgements

References

[Castaneda and Suquet 1997] P. P. Castaneda and P. Suquet, "Nonlinear composites", *Adv. Appl. Mech.* **34** (1997), 171–302.

[Clayton and McDowell 2004] J. D. Clayton and D. L. McDowell, "Homogenized finite elastoplasticity and damage: theory and computations", *Mech. Mater.* **36**:9 (2004), 799–824.

[Cluni and Gusella 2004] F. Cluni and V. Gusella, "Homogenization of non-periodic masonry structures", *Int. J. Solids Struct.* **41**:7 (2004), 1911–1923.

[Dowling 1993] N. E. Dowling, *Mechanical behavior of materials: engineering methods for deformation, fracture, and fatigue*, Prentice-Hall, Englewood Cliffs, NJ, 1993.

[Du and Ostoja-Starzewski 2006a] X. Du and M. Ostoja-Starzewski, "On the scaling from statistical to representative volume element in thermoelasticity of random materials", *Networks and Heterogeneous Media* **1**:2 (2006), 259–274.

[Du and Ostoja-Starzewski 2006b] X. Du and M. Ostoja-Starzewski, "On the size of representative volume element for Darcy law in random media", 2006. P. Roy. Soc. Lond. A Mat.

[Dvorak and Bahei-El-Din 1987] G. J. Dvorak and Y. A. Bahei-El-Din, "A bimodal plasticity theory of fibrous composite materials", *Acta Mech.* **69**:1-4 (1987), 219–241.

[Hazanov 1998] S. Hazanov, "Hill condition and overall properties of composites", *Arch. Appl. Mech.* **68**:6 (1998), 385–394.

[Hazanov and Huet 1994] S. Hazanov and C. Huet, "Order relationships for boundary-conditions effect in heterogeneous bodies smaller than the representative volume", *J. Mech. Phys. Solids* **42**:12 (1994), 1995–2011.

[He 2001] Q. C. He, "Effects of size and boundary conditions on the yield strength of heterogeneous materials", *J. Mech. Phys. Solids* **49**:11 (2001), 2557–2575.

[Hill 1950] R. Hill, *The mathematical theory of plasticity*, Clarendon Press, Oxford, 1950.

[Hill 1963] R. Hill, "Elastic properties of reinforced solids: some theoretical principles", *J. Mech. Phys. Solids* **11**:5 (1963), 357–372.

[Huet 1990] C. Huet, "Application of variational concepts to size effects in elastic heterogeneous bodies", *J. Mech. Phys. Solids* **38**:6 (1990), 813–841.

[Huet 1995] C. Huet, "Bounds and hierarchies for the overall properties of viscoelastic heterogeneous and composite materials", *Arch. Mech.* **47**:6 (1995), 1125–1155.

[Huet 1999] C. Huet, "Coupled size and boundary-condition effects in viscoelastic heterogeneous and composite bodies", *Mech. Mater* **31**:12 (1999), 787–829.

[Jiang et al. 2001] M. Jiang, M. Ostoja-Starzewski, and I. Jasiuk, "Scale-dependent bounds on effective elastoplastic response of random composites", *J. Mech. Phys. Solids* **49**:3 (2001), 655–673.

[Kanit et al. 2003] T. Kanit, S. Forest, I. Galliet, V. Monoury, and D. Jeulin, "Determination of the size of the representative volume element for random composites: statistical and numerical approach", *Int. J. Solids Struct.* **40**:13-14 (2003), 3647–3679.

[Khisaeva and Ostoja-Starzewski 2006] Z. Khisaeva and M. Ostoja-Starzewski, "Mesoscale bounds in finite elasticity and thermoelasticity of random composites", *P. Roy. Soc. Lond. A Mat.* **462**:2068 (2006), 1167–1180.

[Maugin 1998] G. A. Maugin, *The thermomechanics of nonlinear irreversible behaviours: an introduction*, World Scientific, 1998.

[Ostoja-Starzewski 1994] M. Ostoja-Starzewski, "Micromechanics as a basis of continuum random fields", *Appl. Mech. Rev.* **47**:1, Pt. 2 (1994), S221–230.

[Ostoja-Starzewski 1999] M. Ostoja-Starzewski, "Scale effects in materials with random distributions of needles and cracks", *Mech. Mater* **31**:12 (1999), 883–893.

[Ostoja-Starzewski 2000] M. Ostoja-Starzewski, "Universal material property in conductivity of planar random microstructures", *Phys. Rev. B* **62**:5 (2000), 2980–2982.

[Ostoja-Starzewski 2002] M. Ostoja-Starzewski, "Towards stochastic continuum thermodynamics", *J. Non-Equil. Thermodyn.* **27**:4 (2002), 335–348.

[Ostoja-Starzewski 2005] M. Ostoja-Starzewski, "Scale effects in plasticity of random media: status and challenges", *Int. J. Plast.* **21**:6 (2005), 1119–1160.

[Ostoja-Starzewski 2006] M. Ostoja-Starzewski, "Material spatial randomness: from statistical to representative volume element", *Probab. Eng. Mech.* **21**:2 (2006), 112–132.

[Ostoja-Starzewski and Castro 2003] M. Ostoja-Starzewski and J. Castro, "Random formation, inelastic response, and scale effects in paper", *Philos. T. Roy. Soc. A* **361**:1806 (2003), 965–985.

[Ostoja-Starzewski and Wang 1989] M. Ostoja-Starzewski and C. Wang, "Linear elasticity of planar Delaunay networks: random field characterization of effective moduli", *Acta Mech.* **80**:1-2 (1989), 61–80.

[Sab 1992] K. Sab, "On the homogenization and the simulation of random materials", *Eur. J. Mech. A:Solids* **11** (1992), 585–607.

[Suquet 1997] P. Suquet, *Continuum micromechanics*, CISM Courses and Lectures **377**, Springer, Vienna, 1997.

[Ziegler 1983] H. Ziegler, *An Introduction to thermomechanics*, North-Holland, Amsterdam, 1983.

WEI LI: email_liwei@yahoo.com
Department of Mechanical Engineering, McGill University, Montréal, QC, H3A 2K6, Canada

MARTIN OSTOJA-STARZEWSKI: martinos@uiuc.edu
Mechanical Science and Engineering, University of Illinois at Urbana-Champaign, Urbana, IL 61801, United States
http://www.mie.uiuc.edu/research/martinos